UV STELLAR OCCULTATION MEASUREMENTS OF NIGHTTIME EQUATORIAL OZONE

G. R. Riegler*+

Jet Propulsion Laboratory, Pasadena, California 91103

S. K. Atreya*, T. M. Donahue*, S. C. Liu, B. Wasser

Department of Atmospheric and Oceanic Science, Space Physics Research Laboratory
The University of Michigan, Ann Arbor, Michigan 48109

J. F. Drake*

Lockheed Palo Alto Research Laboratory, Palo Alto, California 94304

Abstract. The Princeton University Ultraviolet Spectrometer-Telescope on the NASA Orbiting Astronomical Observatory Copernicus was used for stellar occultation measurements of atmospheric ozone. Two sets of observations of the target star β-Cen were carried out on 26 July 1975 and 13-14 June 1976 at wavelengths from 2550Å to 3100Å. After unfolding of the data, ozone density profiles near the equator within 3 hours of local midnight were obtained at altitudes from 47 to 114 km. A secondary maximum at 97 km has been observed in both sets of data. The ozone density between 47 and 75 km is a factor of 2 to 3 times as large as current models predict. At the lower boundary, about half the ozone destruction should be caused by NO_x and ClO_x. Above 55 km, virtually all loss is due to HO_x. These results suggest an overestimate of HO_x and ClO_x loss processes or a serious underestimate of the O_x production rate. A minimum in O_3 density near 87 km and a maximum at about 97 km are probably caused by reactions of O_3 with atomic hydrogen and maximum nocturnal O_3 production near 97 km.

Observation Technique

The stellar occultation technique for measurements of atomic species from satellites has been used and described by a number of researchers [Hays and Roble, 1973; Riegler et al., 1976; Atreya et al., 1976]. In the usual applications of the occultation method, the line-of-sight to the star crosses the limb of the earth during a time interval of approximately 10 to 25 seconds depending on the satellite orbit and the atmospheric species observed. In the observations to be discussed here, an observing geometry in which the line-of-sight grazes the earth's limb without actually being occulted by the disc is used. Typical observing times for this approach are 200-300 seconds.

The orbit of the NASA Orbiting Astronomical Observatory OAO-3 Copernicus is nearly circular with 745 km altitude and 35° inclination. These orbital parameters are very favorable for occultation measurements since they permit long occultation times during each orbit, and also reliable long-term predictions of suitable future occultation times.

The OAO-3 star tracker is programmed to track on a portion of the light entering the telescope; another portion is split off to the UV spectrometer. Since the star tracker uses visible light and the spectrometer senses UV light, refraction effects and possible guidance problems limit the range of occultation geometries to tangent altitudes above approximately 47 km.

The star tracker design also restricts occultation measurements to nighttime observations when the point of minimum tangent altitude (i.e., the "tangent point") is within three hours of local midnight. These restrictions and some engineering constraints limit applications of the limb-grazing method from OAO-3 to one or two observations per star per year.

The minimum tangent altitude during each orbit varied by approximately 10 km per orbit because of the precession of the ascending node of the OAO-3 orbit. This means that the observing wavelength for each orbit had to be selected to optimize absorption by atmospheric ozone, i.e., to obtain optical depths between 0.03 and 5. This range of optical depths was chosen so as to minimize the effects of uncertainties in the background and unattenuated counting rates. The set of observations, therefore, consists of a sequence of orbits with overlapping altitude ranges and usually different observing wavelengths between 2550Å and 3100Å. The actual data collection during each orbit extended over 240 seconds (limited by the on-board data storage capacity for the observations discussed here). The 1975 measurements were carried out within 25 minutes of local midnight at the tangent point, while the 1976 measurements extended over the range from 0100 to 0300 hours local time.

*Guest Investigator with the Princeton Telescope on the Copernicus satellite which is sponsored by the National Aeronautics and Space Administration.

+National Academy of Science/National Research Council Senior Resident Research Associate.

Paper number 7L0171.

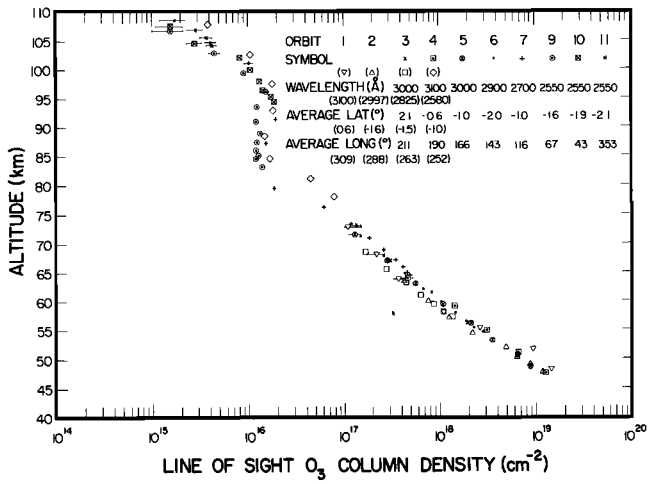

Figure 1. Line of sight ozone column density from the 1975 and 1976 stellar occultation measurements of β-Cen. Wavelengths and average latitudes and longitudes shown in the parenthesis are for the 1975 observations. Error bars of one standard deviation length are shown only when the error exceeds 10%.

Data Analysis

Examples of the data obtained in the 1975 ozone measurements have been presented by Riegler et al. [1976]. The calculation of column densities from the relative attenuation of the net stellar flux signal is readily obtained after compensation for the small effect of Rayleigh scattering. Since the bandpass of the OAO-3 Ultraviolet Spectrometer is narrow, typically 0.06-0.08Å, integration over a finite wavelength band is not necessary.

For the conversion from optical depth of column density we have used the ozone abosrption cross sections tabulated by Ackerman [1971]. According to a review presented by Hudson [1974], these absorption cross sections can be assumed to have an absolute accuracy of better than 5%. The star, β-Cen, was selected as a light source because previous study had shown its spectrum to be free of structure in the wavelength range of interest in our observations. Furthermore, the O_3 absorption cross section as measured with 0.1Å resolution varies smoothly in the wavelength region surveyed.

Figure 1 shows ozone column densities as a function of tangent altitude for the July 1975 and June 1976 observations. The relative statistical uncertainty of the calculated column densities, which includes uncertainties in the unattenuated source response and in the instantaneous detector background rate is shown only when it exceeds 10%. As shown in Figure 1, the various sets of data have been obtained with different observing wavelengths and at different times. However, in all data sets the column densities decrease more or less exponentially up to about 85 km, but abruptly change in shape at that altitude, showing a secondary maximum near 97 km tangent altitude before decreasing again.

The relation between the line-of-sight column density and the local ozone density is given by the Abel integral which can be readily inverted analytically. In our computations we have used two approaches: quadratic or exponential local fits to the column density profile [cf., Roble and Hays, 1972], and a numerical iterative procedure [Wasser, 1975]. The former method introduces local smoothing which depends on the number of data points used. The latter method can, with certain sets of input data, result in non-physical density profile features. At altitudes below approximately 85 km, a simple Chapman-factor conversion may also be used as a verification of the more elaborate Abel integral inversion technique.

Calculations with the above-mentioned inversion methods yield comparable results for the ozone density profiles which reflect the spread in the column density profiles given in Figure 1. Figure 2 shows the range of resulting ozone density profiles. The statistical accuracy of the data and the systematic accuracy of the numerical inversion method for the majority of data below 100 km is such that the density is reliable to within ± 5% and the altitude to ± 0.5 km. The range of ozone densities shown in Figure 2 reflects variations from orbit to orbit as functions of time and geographic location near the equator. The densities can then be compared with average theoretical predictions.

Model Calculations

The model O_3 density profile plotted in Figure 2 was obtained with a diurnal model assuming currently accepted rate constants [Hampson et al., 1977; Margitan, 1977], such as, for example

$$OH + HO_2 \rightarrow H_2O + O_2, \quad k = 2 \times 10^{-11} cm^3 s^{-1} \quad (1)$$

$$O + HO_2 \rightarrow OH + O_2, \quad k = 3 \times 10^{-11} cm^3 s^{-1} \quad (2)$$

The Cl_x volume mixing ratio was assumed to be 2.1 ppb and a tropical model atmosphere was adopted containing 20% more O_2 than the midlatitudes spring and fall model [U.S. Standard Atmosphere Supplements, 1966]. In Figure 3, the O_x loss rates per day due to dominant processes between 40 and 80 km are plotted.

We divide our discussion into two parts, below 75 km and above it. Below about 75 km the experimental O_3 densities are higher than those in the model by a factor of 2 to 3. This is disturbing, since the dominant sink for O_x ($O_3 + O + O(^1D)$) above 55 km is catalytic removal by OH, HO_2, and H while the ClO_x and NO_x cycles should become almost equally effective as the HO_x cycles at 47 km. Throughout the entire altitude regime below 75 km, photochemistry should dominate transport phenomena in determining O_x densities. This discrepancy between theory and observation extends into a region where ClO_x and NO_x destruction of O_x becomes as important as HO_x destruction. If the O_3 data are accepted as valid, either the HO_x and some combination of the ClO_x and NO_x loss processes are all fortuitously overestimated or the O_x production rate is underestimated.

Above 75 km we have used the recently measured [Clyne, 1974] temperature dependence rate for the reaction

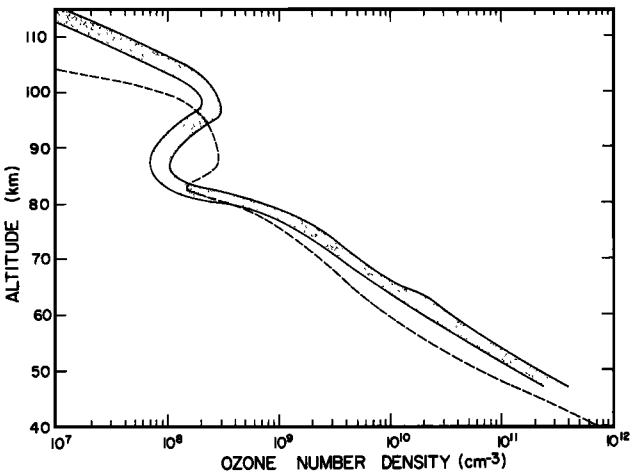

Figure 2. Ozone density profile deduced from the 1976 observations. The shaded area shows the spread in the ozone densities from orbit to orbit. Theoretical model calculation results are shown by the dashed line.

$$H + O_3 \rightarrow OH + O_2 \qquad (3)$$

of $1.23 \times 10^{-10} \exp(-562/T)$. At 180°K the rate of this reaction is a factor of 5 smaller than the value of 2.6×10^{-11} [Hampson et al., 1973] used in an analysis of O_3 data previously published [Riegler et al., 1976]. Since reaction (3) is the dominant loss process for O_3 above 80 km at night, the result is an O_3 bulge above 90 km. The agreement between the model and observed profiles above 80 km is qualitatively good, but an altitude discrepancy of about 5 km exists and this we do not understand.

In fact, the discrepancy between model and observed O_3 densities would effectively disappear at all altitudes if the observed profiles could be shifted downward about 5 km, or atmospheric density increased by about a factor of 2 in the model calculations. Given the geometry of the occultation exercises and the fact that a 5 km error in altitude of the tangent ray height would entail about a 30 sec error in timing and no more than a 2 sec error is expected, we have abandoned this explanation of the discrepancy after a painstaking study of the tracking data. The possible time uncertainty of 2 sec corresponds to an uncertainty in the instantaneous tangent altitude of less than 0.5 km for the lowest altitude data points of each orbit, and less than 1 km for the highest altitude data points. Moreover, a factor of 2 increase in the O_2 density in the homosphere appears unlikely. An equatorial radius of 6378.15 km was used in the data reduction.

The O_3 densities determined in our occultation studies agree well with those measured by Hilsenrath [1974] below 67 km near the equator in a rocket-borne chemiluminescent experiment. They disagree seriously with the data of Hays and Roble [1973] obtained from stellar occultation studies using OAO-2. The geometry of this observation did not permit the long integration time available using the limb grazing technique. The structure in the high-altitude O_3 profile has been deduced previously by Evans and Llewellyn [1970] who analyzed $O_2(^1\Delta)$ and $O_2(^1\Sigma)$ airglow data obtained in sounding rocket experiments in terms of O_3 photolysis. Noxon [1975] deduced similar nighttime ozone profiles above 80 km by observing the twilight enhancement in $O_2(^1\Sigma)$ airglow emission. Quantitatively the Noxon O_3 values, which are somewhat indirectly inferred and are obtained at high latitudes are lower than those reported here. The equatorial observations of $O_2(^1\Delta_g)$ emission by Han et al. [1973] present a more difficult problem of reconciliation since their 1.27 μm emission peak occurred at 80 ± 5 km. Mass spectrometer measurements of ozone between 90 and 110 km by Trinks [1975] have large experimental uncertainties and show no resemblance to the results presented in this paper.

We conclude that there is a serious problem reconciling photochemical models and observed nocturnal O_3 density profiles in the mesosphere. (There is no reason to expect other models to differ significantly from the one we deduce here). We note that a threefold increase in O_3 (or O_x) densities above 55 km due to a decrease in the HO_x catalyzed O_x recombination rates would require a factor of three decrease in HO_x densities. This would call for a factor of about 30 decrease in H_2O and H_2 in the mesosphere because HO_x density is proportional to the square root of products of $H_2O + H_2$ and $O(^1D)$. If the high O_3 densities reported here are characteristic of the tropics alone a conceivable but extremely unlikely explanation for such low tropical mesospheric HO_x densities would involve a very large flux of sources such as CH_4, H_2O, H_2 from the tropical stratosphere. In analyzing the behavior of O_3 above the mesopause it may be useful to keep in mind the evidence obtained by OGO-VI airglow observations that the eddy diffusion coefficient near 100 km at tropical latitudes may be considerably enhanced compared to its value at higher latitudes [Donahue and Carignan, 1976]. Obviously the discrepancy uncovered here would disappear if the ozone absorption cross section were larger by a factor of 2 to 3 than the presently accepted value.

Acknowledgements. The assistance of Dr. E. S. Barker of Princeton University has been of great help during all phases of this research. We thank Dr. R. J. Cicerone for helpful discussions. This work has been supported by the National Aeronautics and Space Administration under Contract NAS 7-100, Task Order RD-65 #261

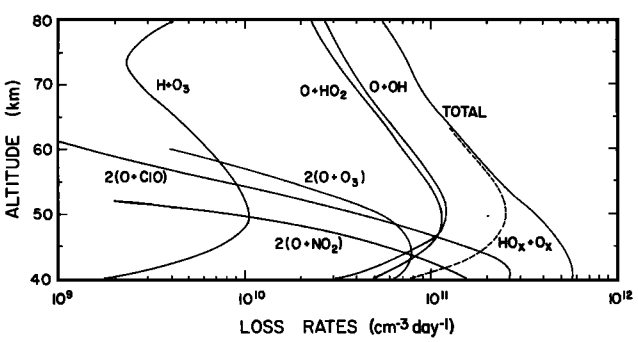

Figure 3. 24 hours integrated loss rates from diurnal model for odd oxygen.

with the Jet Propulsion Laboratory (GRR); NASA Grants NSG 5097 and 5117, and NSF Grant ATM 75-21049 A01 to the University of Michigan; and by the Lockheed Independent Research Program (JFD). We acknowledge the use of the NCAR computing facilities.

References

Ackerman, M., Ultraviolet solar radiation related to mesospheric processes, in Mesospheric Models and Related Experiments, Fiocco, (ed.), Reidel Publishing Company, Dordrecht, Netherlands, 149-159, 1971.

Atreya, S. K., T. M. Donahue, W. E. Sharp, B. Wasser, J. F. Drake and G. R. Riegler, Ultraviolet stellar occultation measurements of the H_2 and O_2 densities near 100 km in the earth's atmosphere, Geophys. Res. Lett., 3, 607, 1976.

Clyne, M. A. A., Technical Report, December, 1974.

Donahue, T. M., and G. R. Carignan, The temperature gradient between 100 and 120 km, J. Geophys. Res., 80, 4565, 1975.

Evans, W. F. J., and E. J. Llewellyn, Molecular oxygen emission in the airglow, Ann. Geophys. 26, 167, 1970.

Hampson, R. F., (ed), D. Garvin, J. T. Herron, R. E. Huie, M. J. Kurylo, A. H. Laufer, H. Okabe, M. D. Sheer and W. Tsang, Survey of photochemical and rate data for twenty-eight reactions of interest in atmospheric chemistry, J. Phys. Chem. Ref. Data, 2, 267-312, 1973.

Hampson, R. F., D. Garvin, M. J. Kurylo, R. E. Huie and W. Tsang, Rate constants for NO_x reaction and those of $O(^1D)$ interest in stratospheric chemistry, prepared for the Laboratory Measurements Committee, NASA CFM Assessment, 1977.

Han, R. Y., L. R. Megill and C. L. Wyatt, Rocket observation of the equatorial $O_2(^1\Delta_g)$ emission after sunset, J. Geophys. Res., 78, 6140-6149, 1973.

Hays, P. B., and R. G. Roble, Observation of mesospheric ozone at low latitudes, Planet. Space Sci., 21, 273, 1973.

Hilsenrath, E., quoted in Observations of the global structure of the stratosphere and mesosphere with sounding rockets and with remote sensing techniques from satellites, in Structure and Dynamics of the Upper Atmosphere, F. Verniani, (ed.), Elsevier, Amsterdam, Netherlands, 187, 1974.

Hudson, R. D., Absorption cross sections of stratospheric molecules, Can J. Chem., 52, 1465, 1974.

Margitan, J. J., HO_x reaction rates, prepared for the Laboratory Measurements Committee, NASA CFM Assessment, 1977.

Noxon, J. F., Twilight enhancement in $O_2(b^1\Sigma_g)$ airglow emission, J. Geophys. Res., 80, 1370, 1975.

Riegler, G. R., J. F. Drake, S. C. Liu, and R. J. Cicerone, Stellar occultation measurements of atmospheric ozone and chlorine from OAO-3, J. Geophys. Res., 81, 4997, 1976.

Roble, R. G., and P. B. Hays, A technique for recovering the vertical number density profile of atmospheric gases from planetary occultation data, Planet. Space Sci., 20, 1727, 1972.

Trinks, H., Ozone measurements between 90 and 110 km by mass spectrometer, Geophys. Res. Lett., 2, 99, 1975.

Wasser, B., Latitudinal dependence of atomic oxygen density between 90 and 120 km as derived from OGO-VI observations of the 5577Å nightglow, Ph.D. Thesis, University of Pittsburgh, 1975.

(Received February 18, 1977;
accepted March 18, 1977.)